Supporting Information

Mimicking the Microbial Oxidation of Elemental Sulfur with a Biphasic Electrochemical Cell

Marco F. Suárez-Herrera,*[a],[b] Alonso Gamero-Quijano,[a],[d] José Solla-Gullón,[c] Micheál D. Scanlon*[a],[d]

[a] The Bernal Institute, University of Limerick (UL), Limerick V94 T9PX, Ireland.

[b] Departamento De Química, Facultad De Ciencias, Universidad Nacional De Colombia, Cra 30 # 45-03, Edificio 451, Bogotá, Colombia.

[c] Instituto de Electroquímica, Universidad de Alicante, Ap.99, E–03080, Alicante, Spain.

[d] Department of Chemical Sciences, School of Natural Sciences, University of Limerick (UL), Limerick V94 T9PX, Ireland.

Corresponding authors:

*E-mail: mfsuarezh@unal.edu.co

*E-mail: micheal.scanlon@ul.ie

S1. Experimental methods

S1.1 Materials. All chemicals were used as received without further purification. All aqueous solutions were prepared with ultrapure water (Millipore Milli-Q, specific resistivity 18.2 MΩ·cm). Bis(triphenylphosphoranylidene) ammonium chloride (BACl, 97%) and lithium tetrakis(pentafluorophenyl)borate diethyletherate ([Li(OEt$_2$)]TB) were obtained from Sigma-Aldrich and Boulder Scientific Company, respectively. Bis(triphenylphosphoranylidene)ammonium tetrakis(pentafluorophenyl)borate (BATB) was prepared by metathesis of equimolar solutions of BACl and [Li(OEt$_2$)]TB in a methanol-water (2:1 v/v) mixture. The resulting precipitates were filtered, washed, recrystallised from acetone and finally washed 5 times with methanol-water (2:1 v/v) mixture. Lithium chloride (LiCl, ≥95%), lithium hydroxide (≥98%), tetramethylammonium chloride (TMACl, ≥98%), and elemental sulfur (analytical standard) were obtained from Sigma-Aldrich. The organic solvent α,α,α-trifluorotoluene (TFT, 99%) was obtained from Acros Organics. PBS-stabilised 5 nm colloidal AuNP suspensions were purchased from Sigma Aldrich.

S1.2 Cyclic voltammetry (CV) and electrochemical impedance spectroscopy (EIS) at the ITIES. Electrochemical experiments were carried out at the water|α,α,α-trifluorotoluene interface using a 4-electrode configuration (the geometric area of the cell was 1.60 cm^2). To supply the current flow, platinum counter electrodes were positioned in the organic and aqueous phases. The potential drop at the L|L interface was measured by means of *pseudo*-reference silver/silver chloride (Ag/AgCl) electrodes, which were connected to the aqueous and organic phases, respectively, through Luggin capillaries. When 10 mM LiOH was used as an aqueous phase, a standard Ag/AgCl reference electrode separated by a porous junction was used to ensure the signal stability of the reference potential. The Galvani potential difference ($\Delta_o^w \phi$) was attained by assuming the formal ion transfer potential of TMA$^+$ to be 0.311 V [1].

The water|TFT interface was functionalized with a film of AuNPs by means of cyclic voltammetry using electrochemical cell 1 (see Scheme 1 in the main text). Electrochemical impedance spectra were measured using an Autolab PGSTAT204 potentiostat with a frequency response analyzer module (FRA32M) and a 4-electrode electrochemical cell. The AC amplitude was 10 mV and the frequency range was between 0.1 and 1000 Hz. Differential capacitances at different applied voltages were measured using potentiodynamic EIS at 80 Hz and assuming the cell behaves as a series R-C circuit. At this frequency, the contribution of faradic processes is insignificant in the working potential window.

S1.3. Cyclic voltammetry (CV) using the 4-electrode CBPEC configuration. The configuration of the 4-electrode closed bipolar electrochemical cell (CBPEC) used in our study is shown in Scheme 2 of the main text, and an image of the setup is provided in Fig. S2. The poles of the bipolar electrode consisted of two polycrystalline gold electrodes, one immersed in the aqueous phase (P_w) and the other in the organic phase (P_o). Each pole was connected through a copper wire. Two Ag/AgCl wires were used as *pseudo*-reference electrodes, one immersed in the aqueous phase and the other in the organic reference solution (*i.e.,* an aqueous solution of 10 mM LiCl and 1 mM BACl, connected through a Luggin capillary). Two platinum wire electrodes, one in each phase, were used as counter electrodes (driving electrodes). Before each electrochemical measurement, a flame anneal procedure was implemented to eliminate any trace impurities. The potential windows of the polycrystalline gold electrodes acting as P_w and P_o, respectively, were monitored using a multimeter and auxiliary Ag/AgCl *pseudo*-references in each compartment as electrical contacts, while the $\Delta_o^w \phi$ in the 4-electrode CBPEC was scanned from –1.0 to +2.5 V.

S1.4. Numerical simulations. The CVs were simulated assuming a Frumkin isotherm, the kinetics given by the Butler-Volmer equation and the mass transport phenomena were neglected. In summary, the following two differential equations have to be solved simultaneously [2,3]:

$$i_T = \upsilon C - R_S C i_T' + nF\Gamma_{max}\theta'$$

(S1)

$$\frac{d\theta}{dt} = k^0 \left[\frac{C^*}{C^0}(1-\theta)e^{-\frac{\alpha nF}{RT}(\eta+g\theta+R_S i_T)} - \theta e^{\frac{(1-\alpha)nF}{RT}(\eta+g\theta+R_S i_T)} \right]$$

(S2)

where i_T is the current that crosses the interface, R_s the total resistance between the two reference electrodes, θ is the surface fraction coverage, Γ_{max} is the maximum surface coverage (mol·m^2), C is the capacitance of the interface, C^* is the bulk concentration in the aqueous phase of the adsorbed specie, g is the interaction parameter of the Frumkin isotherm, and C^0 is the concentration at the reference state. The prime symbol (′) denotes First Derivative. The other symbols have their conventional meaning. The numerical solution of the kinetic differential equations was done using the following Python code:

```
from scipy.integrate import odeint
from matplotlib.widgets import Slider, Button
import numpy as np
```

```
alpha = 0.5
g=0.5
n=1
F=96470
R=8.314
T=300
v=0.05
C=1e-5
gamma_max=2e-9
k0=100
Cb=1e-3
E0=0.2
Ei=0.3
Ef=-0.3
p=n*F/(R*T)
tf=(Ei-Ef)/v

def sol(g,k0,C,Rs):
    def Adsorp(var,t):
        iT = var[0]
        theta = var[1]
        if t < tf:
            E = Ei - v*t
            s=1
        else:
            E = Ef + v*(t-tf)
            s=-1
        eta=E-E0
        theta_d = k0*(Cb*(1-theta)*np.exp(-alpha*p*(eta+g*theta+Rs*iT))-theta*np.exp((1-
alpha)*p*(eta+g*theta+Rs*iT)))
        id = s*v/Rs-iT/(Rs*C)+(n*F*gamma_max*theta_d)/(Rs*C)
        return [id,theta_d]
    t = np.linspace(0,2*tf,1000)
    var0 = [0,0]
    var = odeint(Adsorp,var0,t)
    E1 = np.linspace(0.3, -0.3,500)
    E2 = np.linspace(-0.3, 0.3,500)
    Ev = np.concatenate((E1, E2), axis=0)
    return Ev, var[:,0]*1e6

y=sol(0,100,1e-5,1)

import matplotlib.pyplot as plt
fig, ax = plt.subplots()
plt.subplots_adjust(left=0.15, bottom=0.35)
L1,=ax.plot(y[0], y[1])
ax.set(xlabel='E (V)', ylabel='i ($\mu$A)')

axcolor = 'lightgoldenrodyellow'
axg = plt.axes([0.15, 0.2, 0.65, 0.03], facecolor=axcolor)
sg = Slider(axg, 'g', -0.1, 0.5, valinit=0, valstep=0.05)

axk0 = plt.axes([0.15, 0.15, 0.65, 0.03], facecolor=axcolor)
sk0 = Slider(axk0, '$lg_{10} k^0$', -2, 2, valinit=2, valstep=0.5)
```

```python
axC = plt.axes([0.15, 0.1, 0.65, 0.03], facecolor=axcolor)
sC = Slider(axC, '$Cx10^6$', 50, 1000, valinit=0, valstep=50)

axRs = plt.axes([0.15, 0.05, 0.65, 0.03], facecolor=axcolor)
sRs = Slider(axRs, 'R', 50, 1000, valinit=1, valstep=50)

def update(val):
    gv = sg.val
    k0v=sk0.val
    Rv=sRs.val
    Cv=sC.val
    k=sol(gv,10**k0v,Cv*1e-6,Rv)
    L1.set_ydata(k[1])
    L1.set_xdata(k[0])
    ax.set_ylim(k[1].min(), k[1].max())
    ax.set_xlim(k[0].min(), k[0].max())
    fig.canvas.draw_idle()

sg.on_changed(update)
sk0.on_changed(update)
sC.on_changed(update)
sRs.on_changed(update)

resetax = plt.axes([0.8, 0.9, 0.1, 0.04])
button = Button(resetax, 'Reset', color=axcolor, hovercolor='0.975')

def reset(event):
    sg.reset()
    sk0.reset()
    sC.reset()
    sRs.reset()
button.on_clicked(reset)

plt.show()
```
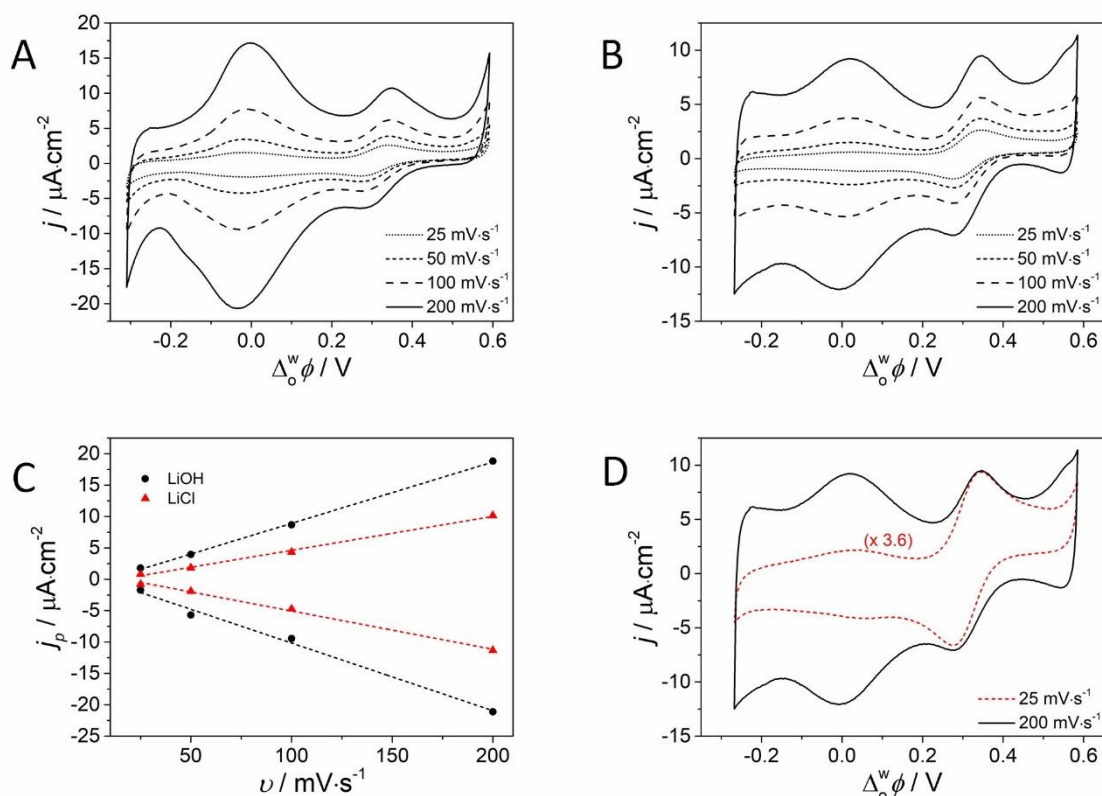
S2. Supporting experimental data

Fig. S1. Adsorption of aqueous anions on the interfacial AuNPs at the polarized L|L interface under aerobic conditions. CVs as a function of scan rate after the addition of 19 μM TMA$^+$ to electrochemical cell 2, see Scheme 1 main text, with **(A)** $x = 0$ and $X = $ Cl$^-$ and **(B)** $x = 0$ and $X = $ OH$^-$. **(C)** Plots of peak current (μA·cm^{-2}) *versus* scan rate (mV·s^{-1}) for the forward and reverse scans of the CVs shown in (A) and (B). **(D)** CVs after the addition of 19 μM TMA$^+$ to electrochemical cell 2, with $x = 0$ and $X = $ OH$^-$, at scan rates of 25 (black line) and 200 mV s^{-1} (red line). All CVs were taken with *iR* compensation.

Fig. S2. Image of the 4-electrode closed bipolar electrochemical cell (CBPEC) used in this study. An H-type electrochemical cell was adapted to perform bipolar electrochemistry under aerobic and anaerobic conditions. An impermeable silicone rubber sheet separated the aqueous and organic compartments. Each pole of the bipolar electrode consisted of a polycrystalline gold electrode, with one immersed in each compartment, denoted P_w in the aqueous phase and P_o in the organic phase, and connected with an electric wire. The composition of the 4-electrode CBPEC configurations used are described in Scheme 2.
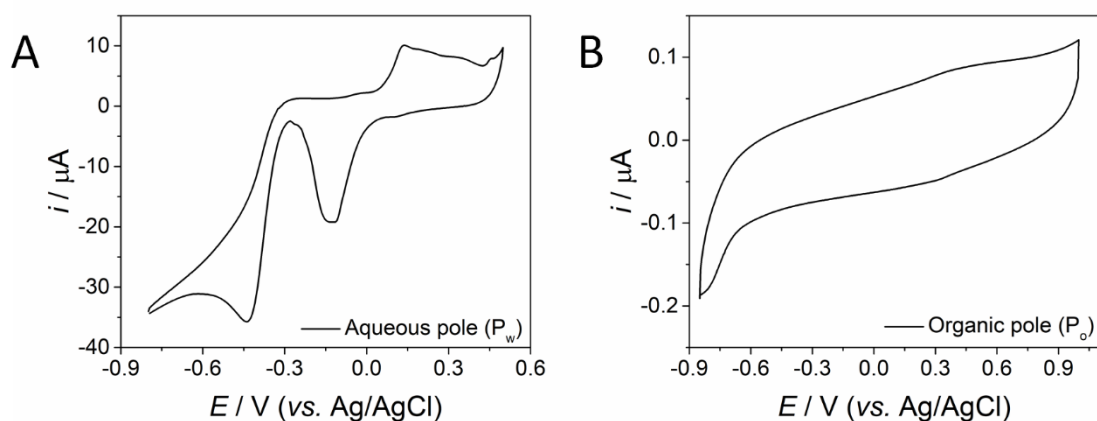
Fig. S3. CVs using three-electrode electrochemical cells of each pole of the CBPEC. (A) CV of the polycrystalline gold electrode acting as P_w recorded 10 mM LiOH. **(B)** CV of the polycrystalline gold electrode acting as P_o with 10 mM S_8 dissolved in the α,α,α-trifluorotoluene (TFT) organic phase. The organic electrolyte salt was 5 mM BATB. All CVs were carried out under aerobic conditions at a scan rate of 25 mV·s^{-1}. In each case, the reference electrode was a Ag/AgCl *pseudo*-reference electrodes and the counter electrode a Pt wire.

S3. Supporting references

[1]   E. Smirnov, P. Peljo, M.D. Scanlon, H.H. Girault, Gold Nanofilm Redox Catalysis for Oxygen Reduction at Soft Interfaces, Electrochim. Acta. 197 (2016) 362–373.

[2]   J.-P. Diard, B. Le-Gorrec, C. Montella, Cinétique électrochimique, Hermann, Paris, 1996.

[3]   N. Eliaz, E. Gileadi, Chapter 12: Electrosorption, 2nd ed., Wiley-VCH Verlag GmbH & Co. KGaA, Weinheim, Germany, 2019.